Electronic Supplementary Material (ESI) for Journal of Materials Chemistry A.

Supplementary Material

Partially unzipped carbon nanotubes for high-rate and stable lithium-sulfur batteries

Yo Chan Jeong, Kunsil Lee, Taehoon Kim, Jae Ho Kim, Jisoo Park, Young Shik Cho, Seung Jae Yang, and Chong Rae Park**

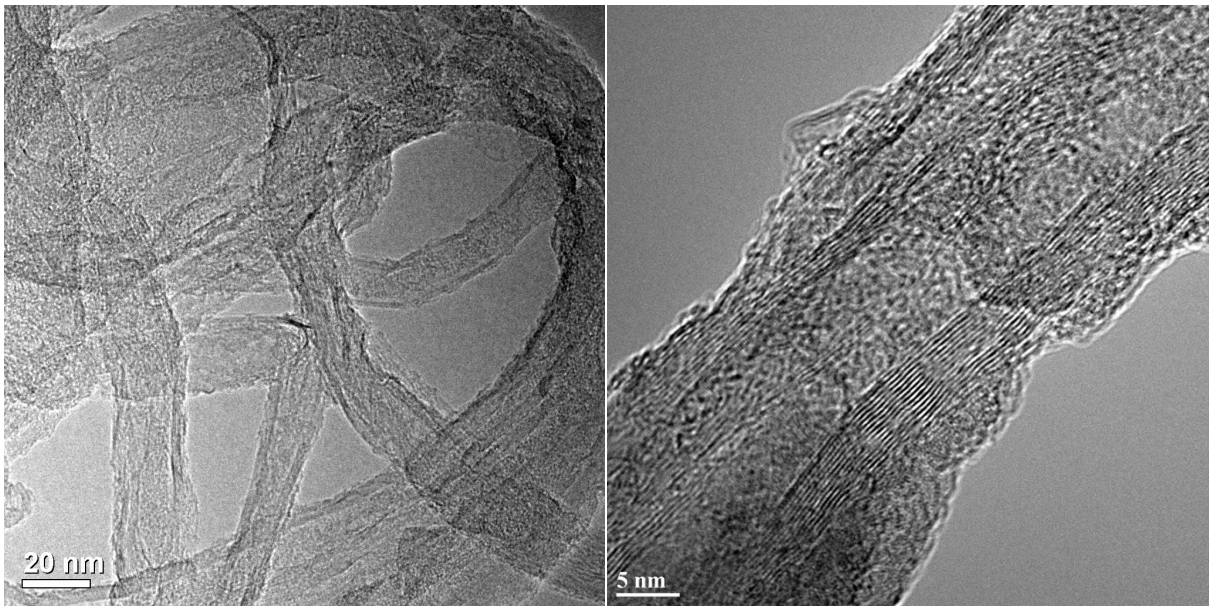

Figure S1. TEM images in two different magnifications of KOH activated MWCNTs without pre-acid treatment.

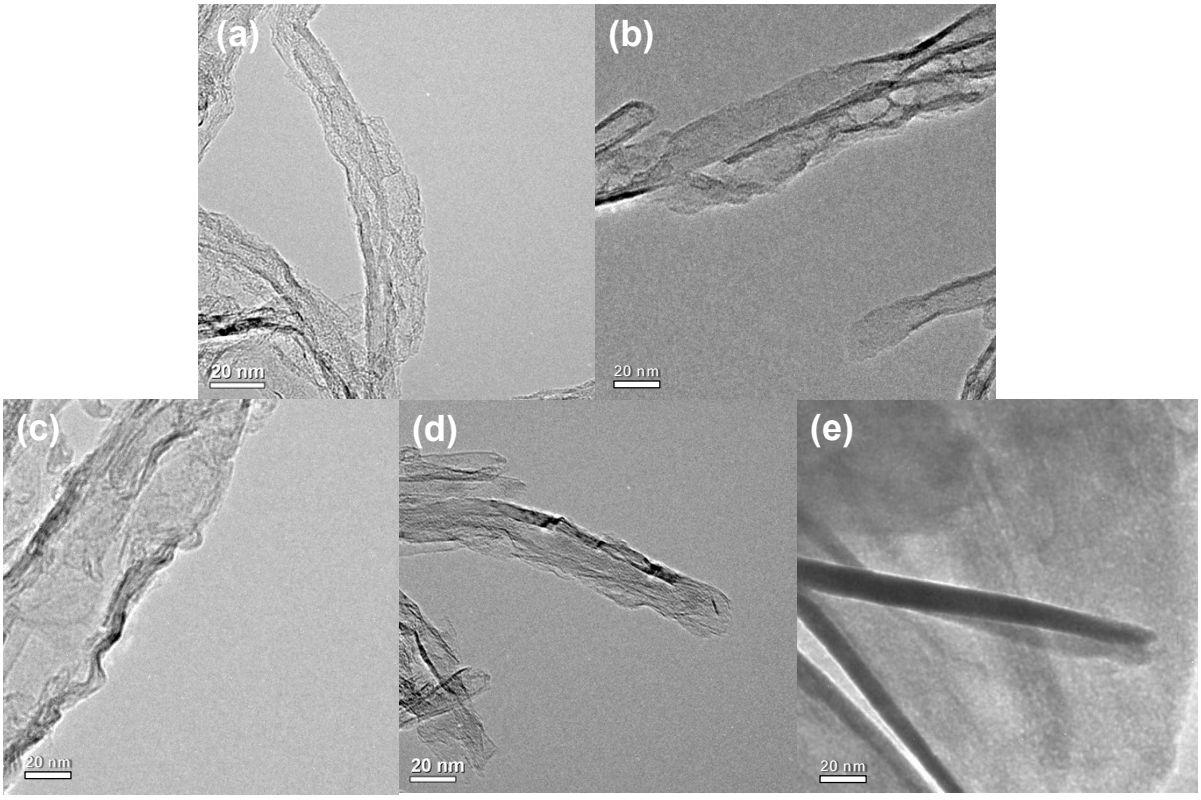

Figure S2. Additional TEM images of UN.CNTs, and UZ.NR: (a) UZ.CNT-1h, (b) UZ.CNT-2h, (c) UZ.CNT-3h, (d) UZ.CNT-6h, and (e) overlapped UZ.NR.

Table S1. Electrical conductivity, thickness and sheet resistance of UZ.CNT-2h and MWCNT film.

Samples	Sheet resistance (ohm sq^{-1})	Thickness (mm)	Electrical conductivity (S/m)
MWCNT	3.4	0.06	4841.0
UZ.CNT-2h	28.4	0.07	503.0

Table S2. BET specific surface area, total pore volume, and average pore size of the samples

Samples	SSA (m^2g^{-1})	V_{total} (cm^3g^{-1})	Avg. pore width (nm)
MWCNT	51.0	0.20	15.8
UZ.CNT-1h	341.6	1.14	13.2
UZ.CNT-2h	473.2	1.15	9.7
UZ.CNT-3h	504.5	0.50	4.0
UZ.CNT-6h	219.2	0.19	3.5
UZ.NR	296.3	0.77	10.4

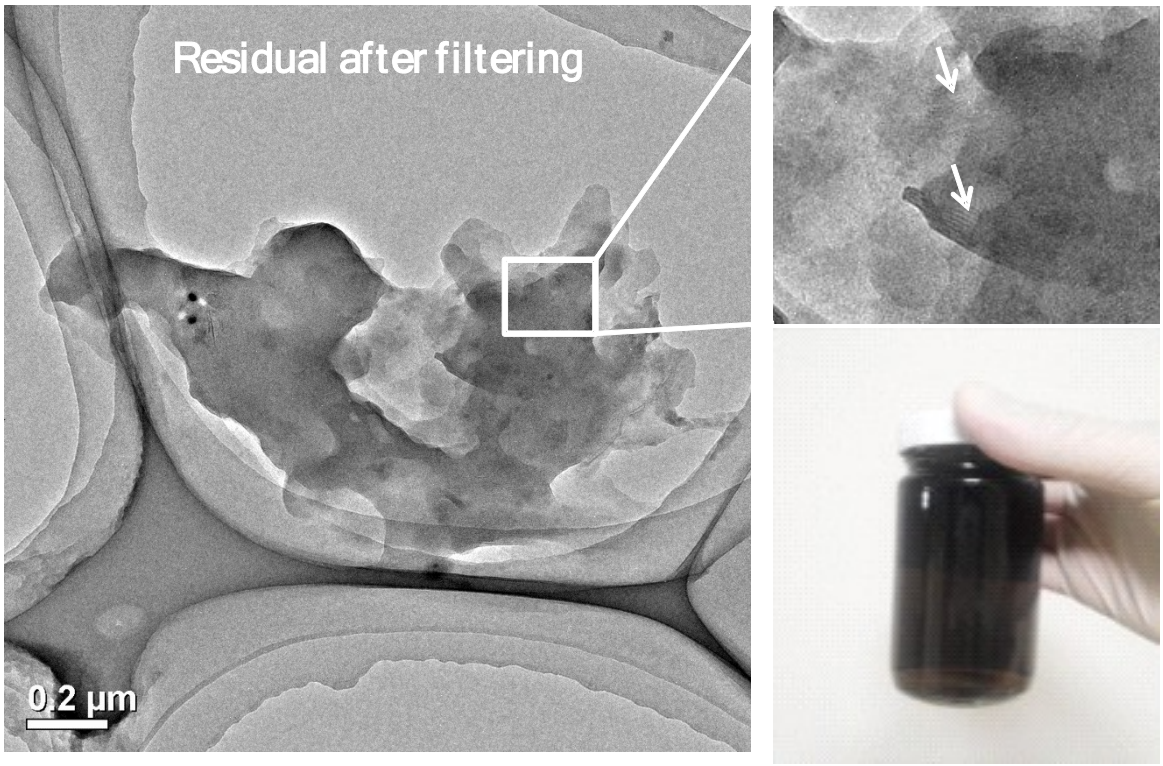

Figure S3. Filtered solution dispersed with small fragmentized carbon particles referred to as acidic carbonaceous fragments (ACFs). This is confirmed by TEM characterization in two different magnifications. ACFs were overlapped together as characterized in precious TEM images.

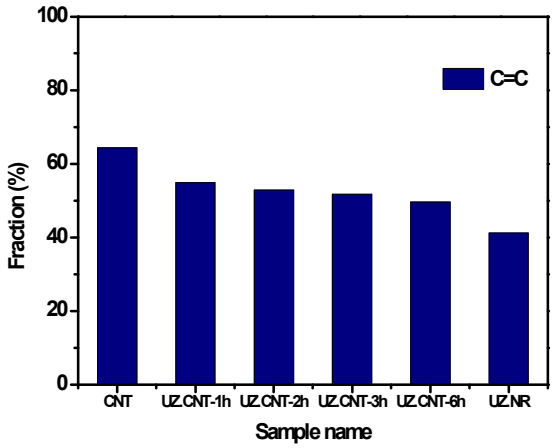

Figure S4. The calculated fractions of C=C from deconvoluted C_{1s} peaks of MWCNT, UZ.CNTs and UZ.NR

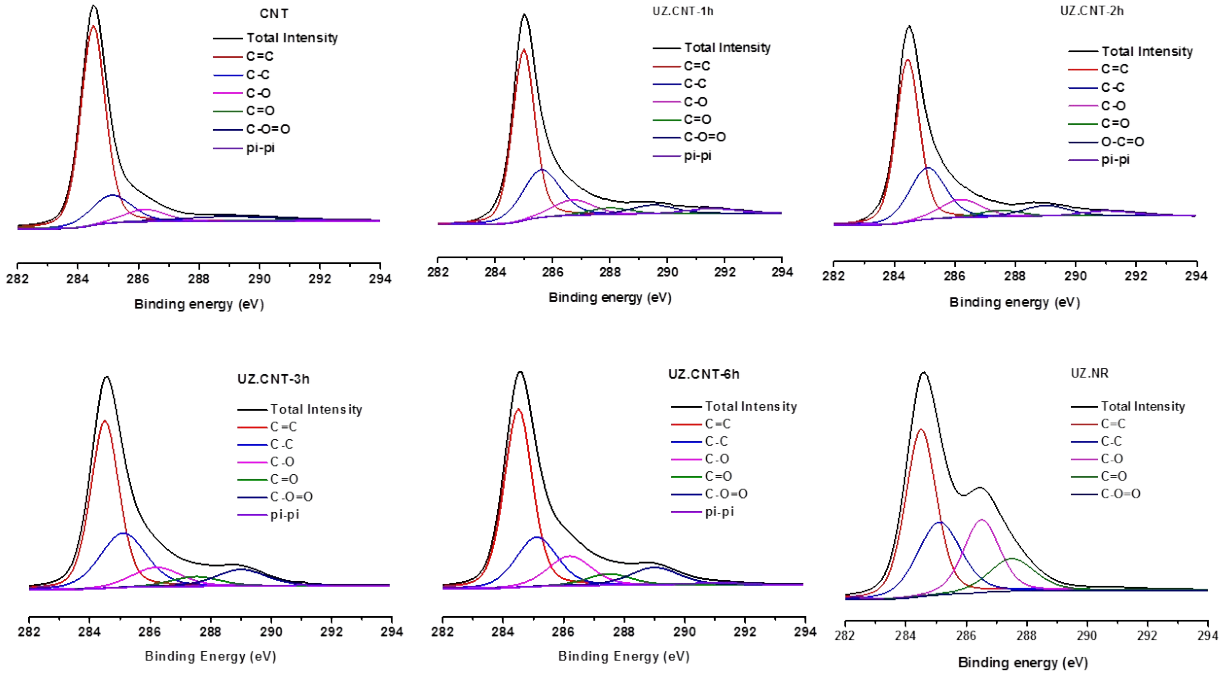

Figure S5. Deconvoluted C_{1s} peaks of MWCNT, UZ.CNTs and UZ.NR

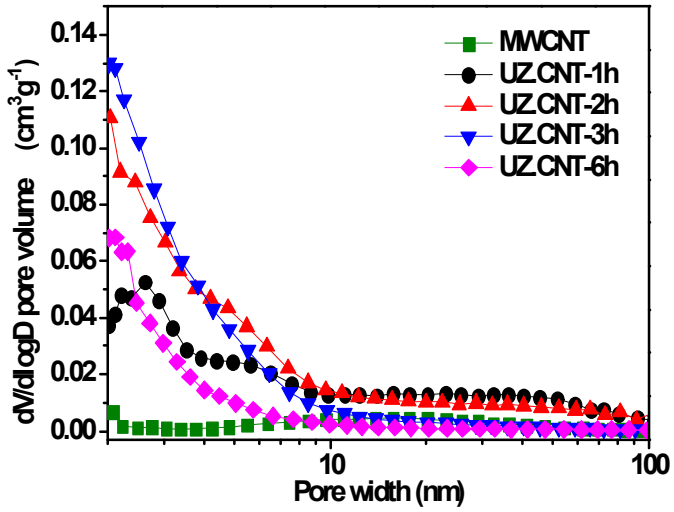

Figure S6. BJH adsorption dV/dD pore volumes of MWCNT, UZ.CNT-1h, -2h, -3h, and -6h confirmed that micro and mesopores were clearly developed by KOH activation.

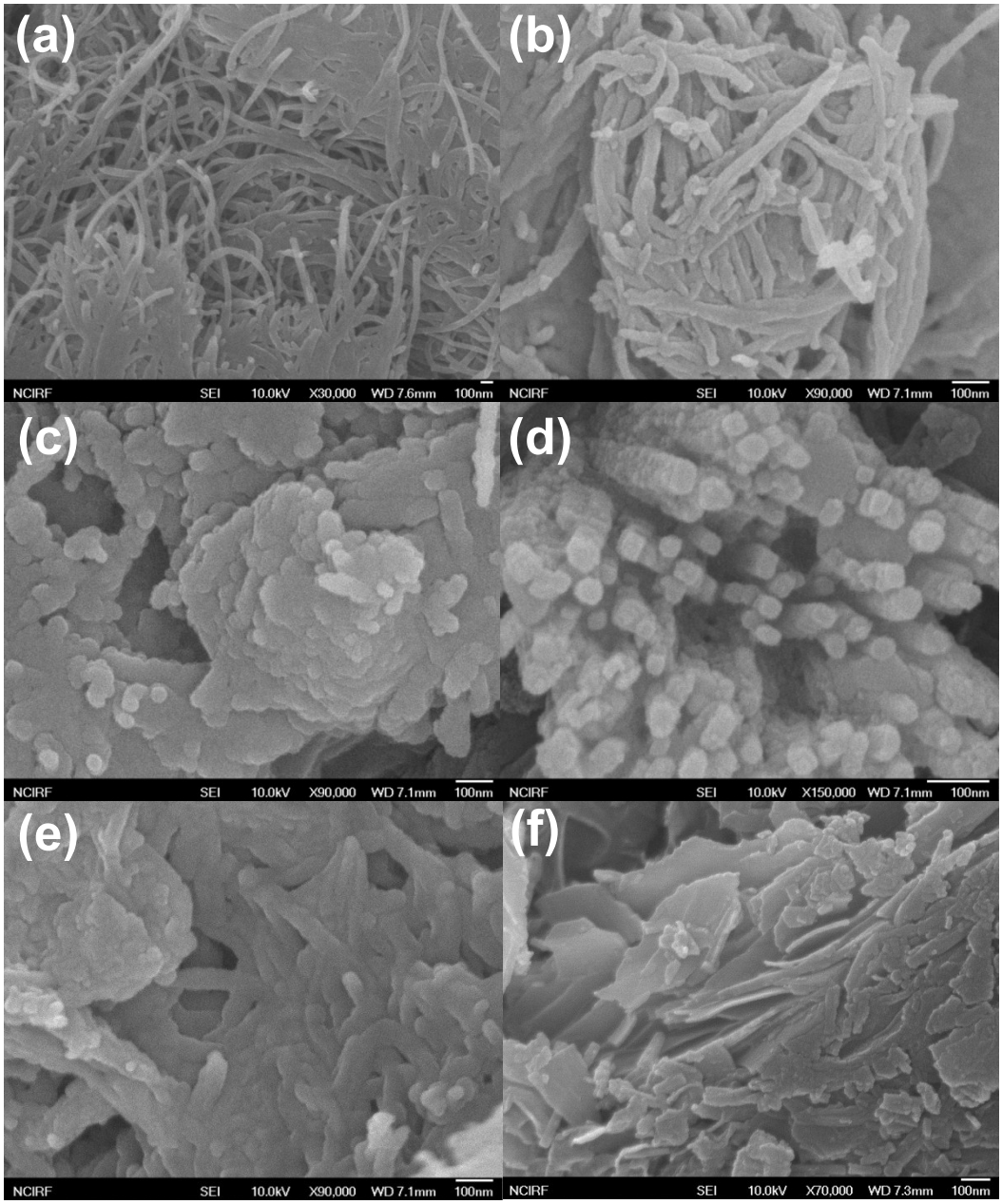

Figure S7. SEM images of (a) MWCNT_S, (b) UZ.CNT-1h_S, (c) UZ.CNT-2h_S, (c) UZ.CNT-3h_S, (d) UZ.CNT-6h_S, and (e) UZ.NR_S composites.

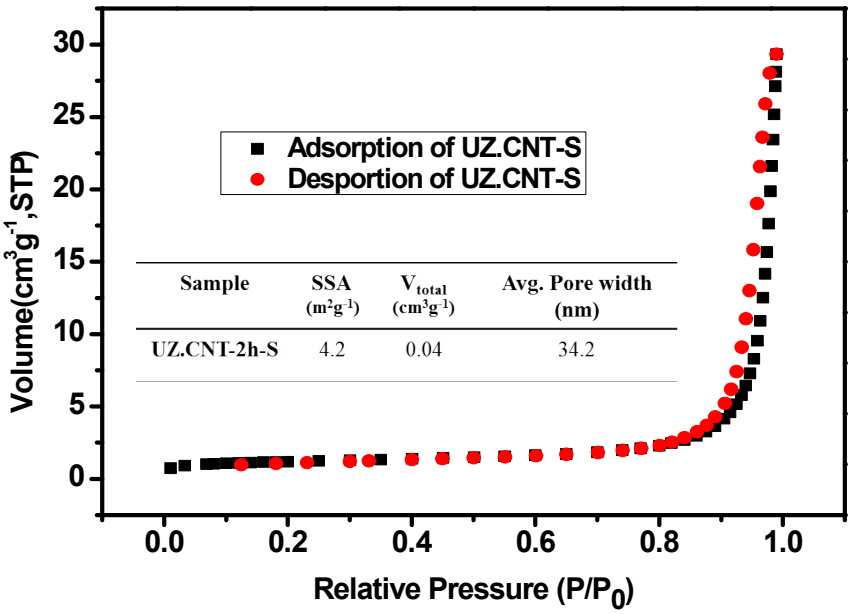

Sample	SSA (m^2g^{-1})	V_{total} (cm^3g^{-1})	Avg. Pore width (nm)
UZ.CNT-2h-S	4.2	0.04	34.2

Figure S8. BET isotherm and calculated specific surface area, total volume and average pore size of UZ.CNT-2h_S composite.

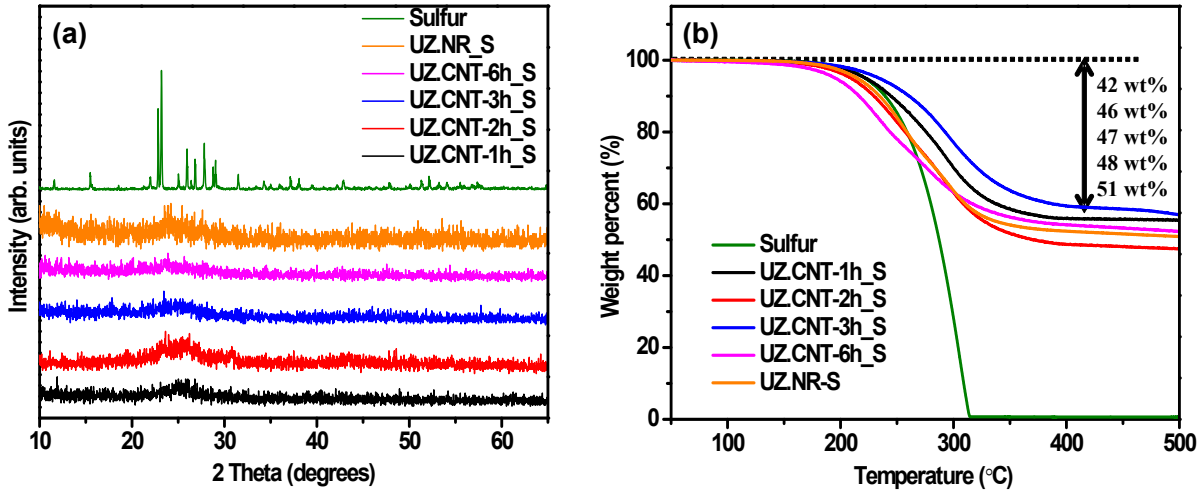

Figure S9. (a) XRD patterns of sulfur and prepared samples. (b) TGA curves of the samples. The average areal sulfur loading in UZ.CNTs was calculated around 2 mg cm^{-2} (1.82-2.10 mg cm^{-2}).

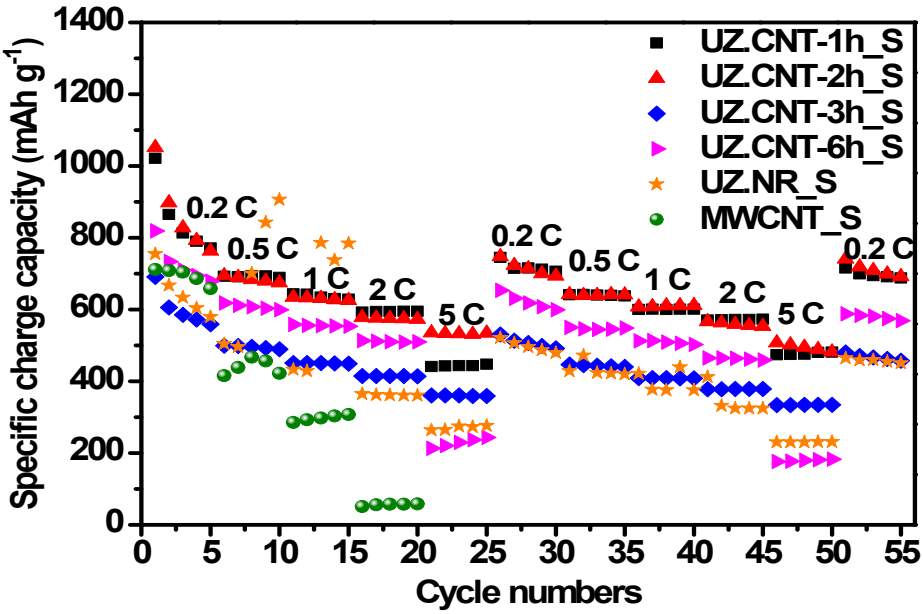

Figure S10. Specific charge capacities of the samples at various charging current densities.

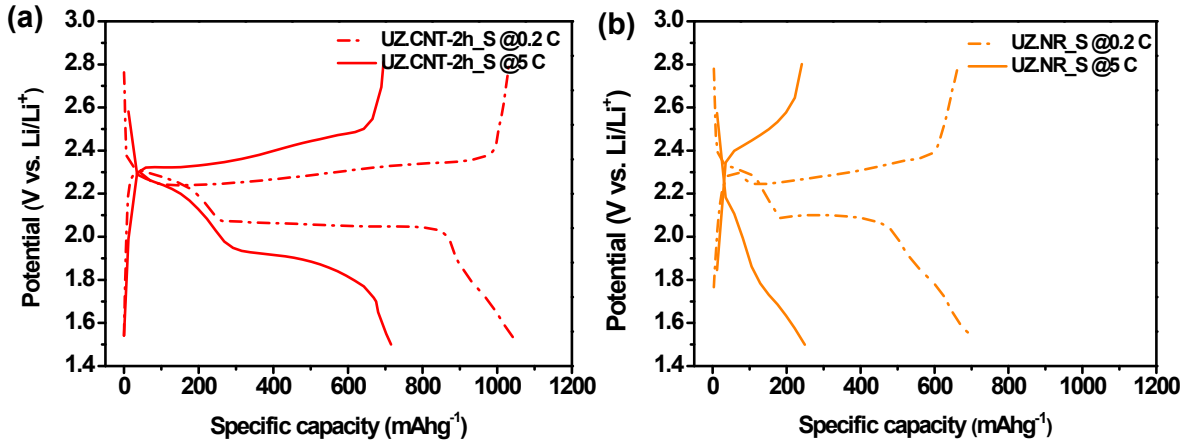

Figure S11. (a) Second charge/discharge profiles of UZ.CNT-2h_S at 0.2 C and 5 C, and (b) the compared charge/discharge profiles of UZ.NR_S at 0.2 C and 5 C.

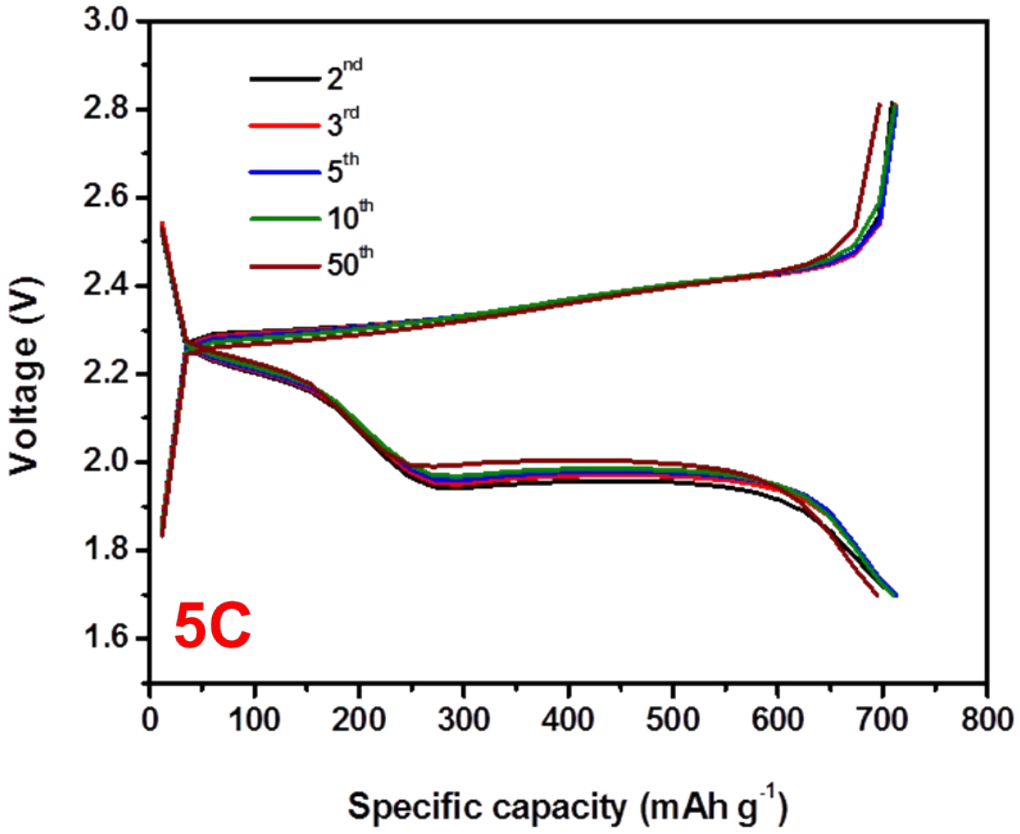

Figure S12. The charge/discharge profiles of UZ.CNT-2h_S at 5 C with 1.7-2.8 V potiential range.

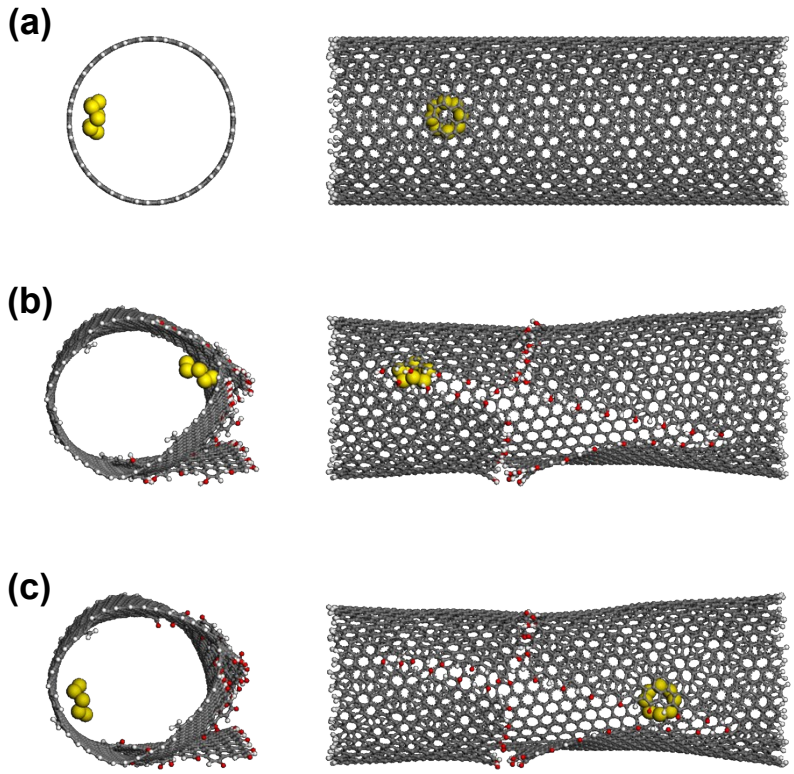

Figure S13. Lowest energy state of (a) CNT_inner, (b) UZ.CNT (-OH), (c) UZ.CNT (-CO).

Table S3. The lowest adsorption energies of sulfur and polysulfide on various carbon matrices from the Monte Carlo simulations

Sorbate	Sorbent	Lowest Energy (kcal mol^{-1})	Valence		Non-bond		
			diagonal terms	cross terms	van der Waals	electrostatic	total
S_8	CNT_outer	-30.088	-6.984	0	-23.104		-23.104
	UZ.NR	-32.474	-6.984	0	-25.489	0	-25.489
	CNT_inner	-36.31	-6.984	0	-29.326	0	-29.326
	UZ.CNT	-40.862	-6.984	0	-33.878	0	-33.878
	UZ.CNT (-CO)	-41.817	-6.984	0	-34.833	0	-34.833
	UZ.CNT (-OH)	-42.761	-6.984	0	-35.777	0	-35.777
	UZ.CNT (-COOH)	-44.17	-6.984	0	-37.185	0	-37.185
S_6^{2-}	CNT_outer	-5.045	8.121	0	-13.166	0	-13.166
	UZ.NR	-6.83	8.121	0	-14.95	0	-14.95
	CNT_inner	-9.039	8.121	0	-17.16	0	-17.16
	UZ.CNT	-14.428	8.121	0	-22.549	0	-22.549
	UZ.CNT (-CO)	-14.513	8.121	0	-22.634	0	-22.634
	UZ.CNT (-OH)	-16.43	8.121	0	-24.551	0	-24.551
	UZ.CNT (-COOH)	-17.704	8.121	0	-25.825	0	-25.825

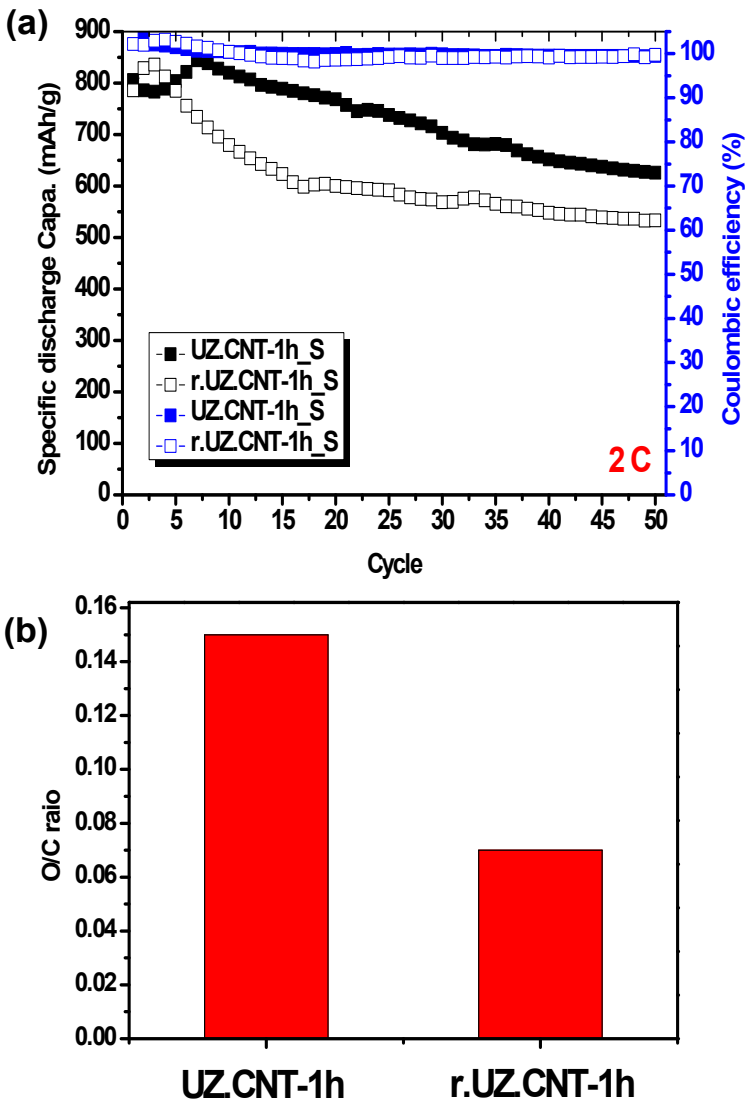

Figure S14. (a) The electrochemical performance of UZ.CNT-1h_S and r.UZ.CNT-1h_S. (b) The decreased O/C ratio of UZ.CNT-1h after the thermal reduction.